

The Application of Microdilatometry to Solvent Swelling of Coals

George D. Cody, Alan Davis, Semih Eser, and Patrick G. Hatcher

Energy and Fuels Research Center and the Fuel Science Program
The Pennsylvania State University, University Park, PA 16802

Introduction

Since Sanada and Honda's initial application of polymer solution theory to solvent swelling to coals (1), many researchers have used solvent swelling as a useful means of obtaining at least qualitative information on the nature of coal's macromolecular network. Solvent swelling analysis exploits the thermodynamic relationship between solvent-coal mixing and elasticity of coal's macromolecular network. As was shown by Flory and Rehner (2), at equilibrium a polymer immersed in an excess of solvent will contain a specific volume of solvent, the total amount of solvent constitutes a thermodynamic balance between the reduction of the free energy due to mixing and the increase in elastic free energy of the network resulting from dilation.

To date, a variety of analytical techniques have been used to measure the equilibrium volume of solvent in coal. No one technique is free of difficulties. Moreover, the specifics of a given research problem may dictate which technique is chosen. In this paper a new means of measuring equilibrium swelled volumes is introduced and compared to values obtained using a more traditional method.

Sanada and Honda's measurements employed a temperature controlled gravimetric device. The equilibrium volume of a solvent (they used pyridine) was determined from the weight gain of approximately 0.1 g of coal measured from the extension of a quartz spring. They report a high degree of precision such that + or - 0.8 mg weight change is detectable. Since their study many other researchers have employed gravimetric methods to determine the equilibrium swelled volume of solvents in coal. Obvious advantages to the gravimetric technique are 1) the high degree of sensitivity and 2) solvent swelling measurements at solvent activities less than 1.0 can be readily obtained. A disadvantage of this technique is that significant condensation of solvent can occur within coal's pore structure. This potential error is dealt with by correcting the gravimetric data assuming that capillary condensation has occurred in pores. Thus prior to swelling the extent of porosity in coals must be known. One problem with this correction, however, is that it has been shown that upon swelling of coal in pyridine significant changes in coal's pore structure take place (3), therefore, a correction based on "dry" pore volume may not be sufficient.

Liotta et. al (4) published a simple technique for measuring the equilibrium volume of solvent in coal by simply measuring the volume expansion of the coal. Green et al.(5) confirmed the accuracy of this technique by comparing results so obtained to those gathered using gravimetric techniques. The advantages of the volumetric technique is that it is rapid, exhibits good

reproducibility, and requires no special equipment. A potential error is that interparticle volume contributes to the total volume of the sample. This potential source for error is typically addressed by using very fine mesh coal particles and assuming that the change in interparticle void volume upon swelling is exactly proportional to the increase in coal's volume upon swelling. The volumetric method enjoys much use by many coal researchers today because of its convenience and high degree of reproducibility.

In addition to these methods there are a variety of other techniques which although fundamentally related to one or the other of the above techniques use significantly different means by which a measurement is obtained. Aida and Squires (6), for example measured the volume expansion of particulate coal using an apparatus similar in concept to a vapor pressure osmometer. They reported that their apparatus gave results which compared well to established techniques and afforded a greater facility in measuring the kinetics of swelling. Cody et. al. (7) used solvent swelling of coal thin sections using the preparation method designed by Brenner (8) and recorded the equilibrium solvent uptake via changes in linear dimension measured parallel and perpendicular to the bedding plane. This method also yielded values comparable to bulk values and was especially well suited for studying effects of residual network strain and subsequent strain relaxation upon the swelling behavior of un-extracted coals.

This paper will focus on the application of a high sensitivity microdilatometer for the purpose of measuring linear expansion of coal slabs following immersion in a solvent.

Experimental:

The microdilatometer employed in this study was originally used to study the expansion of particulate coals under gasification conditions (9). Figure 1 is a schematic diagram of the dilatometer. The microdilatometer measures the change in position of a linear variable differential transformer (LVDT) core composed of soft iron. The LVDT is attached directly to a glass probe which rests on top of the sample. The position of the LVDT between two electric coils within the dilatometer is sensitively detected using the principles of mutual inductance. At its most sensitive setting extremely small vibrations in the lab are readily detectable by the dilatometer. Thus, the practical lower limit in measurement without resorting to a vibration dampening table is on the order of 1 μ m. As will be discussed shortly, in the current experiments expansions of coal due to solvent swelling are on the order of hundreds of microns using millimeter scale samples.

Two important modifications to the dilatometer have enabled its use in precisely measuring solvent swelling. First, the dilatometer probe is modified as follows. In place of the solid pyrex probe, a hollow probe with vents at the probe tip has been manufactured. Higher up on the probe lies an access port for a syringe for the purpose of injecting solvent. Second, the entire probe/LVDT assembly weighs approximately 20 g. Using a counter balance it is possible to reduce the effective weight of the probe/LVDT assembly to approximately 100 mg. This weight is just

enough to exceed frictional forces within the system. The error that this force adds to the final expansion value is evaluated as follows. The elastic modulus of coal will be the least at the most swollen state. For solvent swollen coal the elastic modulus (on compression) was measured by Doug Brenner and is in the range of 500 psi (10). The typical compressive stress on the samples in this study are in the range of 5×10^{-2} psi. Using a standard equation for strain for uniaxial compression of a polymeric material (equation 1)(11) we calculate a deviation of the true expanded dimension to be less than one tenth of 1 percent.

$$P = E/3(\lambda - \lambda^{-2}) \quad (1)$$

In equation 1, P = pressure, E = the elastic modulus, and λ is the compression ratio.

The second important aspect of this experiment involves preparation of the samples. Table 1 lists the samples and other pertinent information. Three of the coal samples are vitrains from large coal blocks, the other two are coalified logs. For the purpose of comparing the volume expansion values measured using the microdilatometer with values obtained using a bulk volumetric analysis pyridine extracted (exhaustively) samples were required.

The following sample preparation protocol was applied for solvent swelling using a microdilatometer. Vitrain bands were selected from large particle samples of each coal (in the case of the coalified woods all of the matter is vitrain). Small slabs were cut from each sample using a fixed SiC disc grinding wheel. The initial size of the sample is typically on the order of $1 \times 1 \times 1.5$ mm. To avoid forming microcracks during extraction each slab was first equilibrated with pyridine vapor, typically 1-2 days of equilibration. Following this the samples were immersed in a large excess of pyridine liquid (approximately 10 ml) and gently heated at a temperature of about 40 °C. After no less than 4 days of immersion, the samples were de-swelled by sequential series of dilutions with chlorobenzene, each dilution was 9:1 chlorobenzene to solution by volume. Finally the samples were placed "wet" in a desiccator with a tray of chlorobenzene and allowed to come into equilibrium with chlorobenzene vapor. The "dry" samples were then transferred to a vacuum oven and dried for approximately 1 day. This protocol generally resulted in samples free of microcracks.

Prior to swelling each sample was carefully inspected under the microscope for the presence of microcracks. Only Pittsburgh No. 8 presented major difficulties. Regardless of the amount of time allowed for each step of the preparation protocol, samples of Pittsburgh No. 8 exhibited significant microcracks parallel to the bedding plane. Thus, for this sample a second stage of preparation following extraction was required. Using a binocular microscope, microtweezers, and a razor knife it was possible to carve out apparently microcrack-free regions of the original slabs of this coal.

Sample preparation and solvent swelling protocol applied for bulk volumetric solvent swelling analysis is identical to that described by Liotta et al. (4). Approximately 1.0 g of finely ground, extracted coal is charged into a calibrated centrifuge

tube. An excess of solvent is added and the sample is vigorously shaken to ensure free volume expansion. After 24 hr the equilibrium swelled volume of the sample was measured from the increase in height of the coal-pyridine interface.

The actual solvent swelling analysis using the microdilatometer is straightforward. The prepared sample is placed in the sample cavity and the dilatometer head is placed on top of the sample. From the point that solvent is charged into the probe via a syringe, linear expansion data is continuously recorded. When no further expansion takes place this maximum value is taken to equal the cube root of the coal's equilibrium swelled volume.

Results and Discussion

The size of samples in this study varied from 1.3 to 1.9 mm in the direction parallel to the dilatometer probe. Expansions due to solvent swelling are, therefore, on the order of a 100 to 400 μm . Table 2 gives the comparative results. It is clear that in all cases the linear expansion ratios obtained using microsamples of coal in the microdilatometer are comparable to the cube root of the bulk swelling ratio obtained using the bulk volumetric method. Thus for solvent swelling analysis of small amounts of sample the dilatometer is a reliable tool.

Implications derived from the comparison between the two sets of data are 1) the assumption implicit in volumetric swelling that the increase in the interparticle volume with swelling is proportional to an increase in swelled particle volume is reasonable, 2) the assumption that for vitrinite rich coals the bulk swelling behavior is dominated by the swelling behavior of vitrinite is also supported by this comparison.

The microdilatometer can accurately and precisely measure the dilation of coal during solvent swelling. For cases where only a very small amount of sample is available for analysis this instrument is invaluable. For example, solvent swelling analysis of phytoclasts (organic particles) liberated from organic rich rocks is now readily possible.

References

- 1) Sanada, Y., Honda, H., Fuel, 1966, 48, 295
- 2) Flory, P.J., Rehner, J., J. Chem. Phys., 1944, 12, No.10, 412
- 3) Winans, R., Thiagarajan, P., Energy Fuels, 1988, 2, 358
- 4) Liotta, R., Brown, G., Isaacs, J., Fuel, 1983, 62, 781
- 5) Green, T.K., Kovac, J., Larsen, J.W., Fuel, 1984, 63, 935
- 6) Aida, T., Squires, T.G., ACS Chem. Prepr., Div. of Fuel, 1986, 30, No.1, p.95
- 7) Cody, G.D., Larsen, J.W., Siskin, M., Energy Fuels, 1988, 2, 340
- 8) Brenner, D., Fuel, 1984, 63, 1324.
- 9) Khan, M.R., PhD Thesis, 1985, Pennsylvania State University
- 10) Brenner, D., ACS Chem. Prepr., Div. of Fuel, 1986, 31, No.1, p.17

- 11) Treloar, L. R. G., The Physics of Rubbery Elasticity, 3rd Edition, Clarendon Press, Oxford, 1975

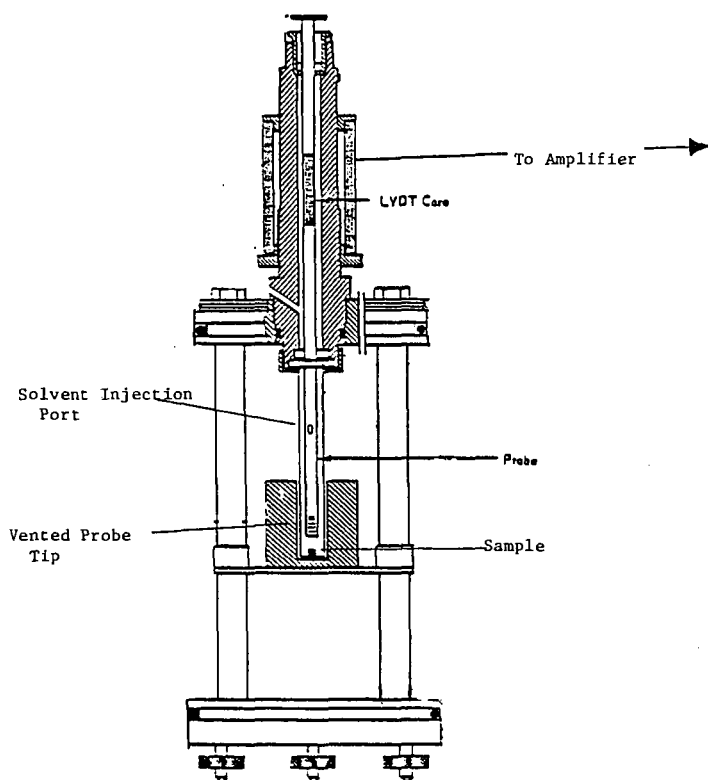


Figure 1: Schematic of microdilatometer modified after Khan, 1985

Table 1 - Coal Samples Studied

<u>SAMPLE</u>	<u>% C</u>	<u>% H</u>	<u>% O</u>	<u>% N</u>	<u>% S</u>	<u>RANK</u>
Smith Seam	70.8	5.0	22.8	0.9	0.5	subbit C
Illinois No. 6	81.9	5.5	9.4	1.4	2.2	Hvb C
Pittsburgh No.8	84.8	5.7	7.4	1.4	0.8	Hvb A
Wyodack/Anderson*	-	-	-	-	-	subbit
Ferron*	78.0	5.3	14.0	1.0	1.7	subbit

* = coalified log

Table 2 - Comparison of Solvent Swelling Results

<u>SAMPLE</u>	<u>Q_r/Q_i</u>	<u>$L_r/L_i(\text{calc})^*$</u>	<u>L_r/L_i^{**}</u>
Smith Seam	1.26	1.08	1.10
Illinois No.6	2.30	1.32	1.29
Pittsburgh No.8	2.30	1.32	1.29
Wyodack/Anderson	1.67	1.19	1.22
Ferron	1.67	1.19	1.19

*linear expansion ratio, the cube root of the bulk swelling ratio Q_r/Q_i .

**linear expansion ratio, measured with microdilatometer

New Applications of Differential Scanning Calorimetry and Solvent Swelling for Studies of Coal Structure

Yongseung Yun, Yoshinobu Otake¹ and Eric M. Suuberg
Division of Engineering, Brown University
Providence, RI 02912

Keywords: Solvent swelling, Differential Scanning Calorimetry, Coal macromolecular structure

Introduction

There have been several reports of structural changes in coal at low temperature (<400°C) indicated by increased mobility of the coal [1] or by crosslinking (associated with the evolution of water and carbon dioxide [2,3]). Since no significant weight loss is normally observed in this low temperature range except moisture and small amount of CO₂, glass transition and/or physical melting have been suspected as responsible for the increased mobility observed in bituminous coals. Some bituminous coals, e.g., Pittsburgh No. 8 coal, are known to contain a considerable amount of thermally extractable mobile phase at temperatures below 400°C [4,5] and thus the role of physical structural changes in releasing this material cannot be ruled out. Recent results on pretreatment of coal for liquefaction by steam, solvent swelling, and preheating have proved that elevated temperatures below those needed for thermal decomposition help enhance the efficacy of the pretreatments, perhaps by promoting greater accessibility of the structure in coal.

Many analytical tools, e.g., GC, MS, TG/FTIR, TG/MS, which focus on gas phase volatiles, are useful for studies involving thermally induced changes in some functional groups of coal whereas FTIR, NMR, Gieseler Plastometry, Dilatometry, and TMA (Thermomechanical Analysis) focus on the study of the char residue with the first two again directed mainly at obtaining functional group information and the last three at obtaining physical structural data. Differential Scanning Calorimetry (DSC) has been used less for the latter purpose, but as will be seen, can be a suitable tool for studying the structural changes involved at low temperatures.

DSC has earlier been used for measurements of the heats of pyrolysis and hydropyrolysis [6-10], as well as for the determination of glass transition temperatures of coal [11,12]. Because of its sensitive nature, DSC is an ideal tool for investigating the thermal changes associated with softening as well as glass transition and thus for identifying the temperatures of significant structural changes. Therefore, DSC has been heavily applied in polymer science and many commercial devices are available. The application of DSC to coal has been hampered by problems caused by weight loss that accompanies most heat effects and also by tar condensation in the DSC cell. Although hermetic sealing of the coal sample is possible, the pressure build-up inside the cell can easily exceed the maximum allowable pressure of the normal sealed capsules (usually 10 atm). This is apparent, considering that at 200°C the vapor pressure of water is already 15.3 atm. Thus it is difficult to measure well-defined heat effects, partly for this reason. Moreover, water evolution can continue up to 300°C, depending on heating rate and sample, and thus overshadow the heat effects due to structural changes below 300°C.

In this paper, we applied DSC in a way such that minute heat effects could be identified by subtracting consecutive DSC scans. Several groups have already applied this type of methodology in helping identify problems with heat capacity measurement [13,14], but did not draw any conclusions concerning the role of structural changes in heat effects. In combination with solvent swelling, which has been also extensively used for characterizing the density of crosslinking in the macromolecular structure of coal, DSC appears to be a powerful tool for evaluating the extent of

¹Present address: Osaka Gas Company, Ltd., Research Center, Osaka, Japan.

thermally induced structural changes.

Experimental

Aliquots of several coal samples, obtained from the Argonne National Laboratory - Premium Coal Sample Program, were analyzed by DSC and solvent swelling techniques. These samples included Pittsburgh No. 8 (-20 mesh), Illinois No. 6 (-20 mesh), Blind Canyon (-20 mesh), Upper Freeport (-100 mesh), and Pocahontas No. 3 (-20 mesh) coals. They were used as-received. Detailed petrographic, chemical, and physical analysis data on these coals can be found elsewhere [15].

Differential Scanning Calorimetry

A DuPont 2910 DSC system with a liquid nitrogen cooling accessory (LNCA-II) was employed in this study. The sample cell was operated under a nitrogen flow rate of 90 ml/min in order to keep the cell free of oxygen during measurement. Aluminum sample pans were generally used in an unsealed mode. This was done by just pushing down the top sample pan cover gently onto the bottom pan containing the coal. Samples were heated from 30°C at 8 °C/min or 30 °C/min. Typically 22-28 mg of sample was used in an experiment. Cooling of the cell between consecutive heating scans normally involved air convection, but several runs were cooled at a controlled rate of 20 °C/min with liquid nitrogen as a cooling medium.

Solvent Swelling

The details of this technique were described earlier [16]. In short, coal samples were placed in constant diameter tubes (3 mm i.d., ca. 5 cm high) and centrifuged at 7500 rpm for 3 min in a roughly 30 cm horizontal rotor (SAVANT HSC-10K high speed centrifuge), after which the initial height of the sample was measured by a caliper. The choice of 7500 rpm was rather arbitrary and selected only to be as high as could be comfortably tolerated by the equipment. Solvent was then added and stirred until a visual check showed the total submergence of coal in solvent. The stirring was repeated frequently (normally 3 times) during the first 30 min following solvent addition. At the desired measurement times, the sample tubes were centrifuged again (7500 rpm for 3 min), the swollen coal height measured, and the solvent replaced with the clean solvent. This assured that the concentration of extractable was not so high as to interfere with the measurement.

Samples (22-28 mg) for solvent swelling were prepared in the DSC at a heating rate of 8 °C/min under a nitrogen flowrate of 90 ml/min. After reaching the desired temperature, each sample was cooled immediately by contacting the bottom of the sample pan with ice or cold water.

Swelling solvents employed (tetrahydrofuran(THF), pyridine) were all reagent grade and were used without any further purification.

Results and Discussion

DSC is a very sensitive technique for determining the difference in heat flow between a sample and a reference material, both heated (or cooled) at a controlled rate. The main purpose in employing DSC here was to determine whether DSC can be used more effectively than it has been, as a tool for examining structural changes in coal, particularly those that occur before pyrolysis. One of the phenomena we were concerned with was the so-called glass transition. The glass transition temperature, T_g , is defined as the temperature at which amorphous polymers transform in structure from the glassy state to liquid/rubbery state. In coal, this transformation has been suggested to appear just before thermal degradation begins [11,12]. Due to the heterogeneity and complexity of constituents involved in coal, a clear-cut determination of T_g in coal has been difficult, as might be

expected.

Figures 1-3 show blank background-subtracted DSC thermograms for three high volatile bituminous coals, i.e., Pittsburgh No. 8, Illinois No. 6, and Blind Canyon coals. Samples were predried inside the DSC up to 150°C just before the first run in Figures 1(a)-3(a). The drying occurred at the same experimental conditions as the following DSC runs. Intermediate oxygen exposure was avoided. Figures 1 through 3 also show difference DSC thermograms for three consecutive scans of the same sample. The general trend for three consecutive scans of a sample in Figures 1(a)-3(a) is that the earlier scans show a slightly more endothermic response above 250°C than do later scans. The sharp initial peaks at ca. 40°C on initial heating do not represent any physically significant heat effects. The general downward direction of the thermograms upon heating represent the effect of heat capacity of coal. The subtraction of a first or second thermogram from a second or third one (as a reference) allows very subtle irreversible changes to be examined. If no irreversible changes were involved, the subtracted spectra would be flat, at a value of zero. In Pittsburgh No. 8 coal, the (1st-3rd) difference thermogram shows significant change in 200-300°C range, while the (2nd-3rd) shows much less change. The reasons for this are discussed below.

Illinois No. 6 and Blind Canyon coals also demonstrate the same behaviors, described above. The peak around 110-120°C in the third scan of Illinois No. 6 coal was due to inadvertent water vapor readsorption from ambient air, which occurred while cooling the sample for the 3rd run in the DSC. This water readsorption peak (up to 150-200°C) helps define the temperature range at which moisture would have influenced the DSC thermogram. The distinct downward peak around 190°C in Blind Canyon coal (Figure 3) was also found to be related to incomplete drying; drying was performed inside the DSC cell at a heating rate of 8 °C/min up to 150°C, which was apparently not sufficient to completely drive off all moisture.

The observations in Figure 1 appear to confirm an earlier suggestion [17] that Pittsburgh No. 8 coal has an irreversible heat effect associated with glass transition around 275°C, while Illinois No. 6 and Blind Canyon coals have a T_g value higher than Pittsburgh No. 8 coal. The transition in Illinois No. 6 coal appears to be centered at around 300°C and that in Blind Canyon coal at 275-300°C. The irreversible heat effect was endothermic (downward in the figures) which is an indication of structural relaxation in the first scan. It must be noted that the transition is irreversible, otherwise it would not be visible in the subtractive technique. We earlier saw an irreversible change in THF swellability at this temperature [17]. This in no way suggests that the glass transition itself is irreversible, but rather that the relaxations that occur with glass transition, are irreversible (vide infra). All three coals exhibited initial agglomeration behavior from ca. 340°C, as observed visually from the coal sample after cooling. Thus the softening of coals, leading to gross agglomeration, has not yet commenced at the observed temperature range of the structural transition that we hypothesize to be a glass transition.

Another noteworthy fact observed in Figures 1(a)-3(a) is the reproducibility of small peaks in the thermograms starting from around 150°C, indicating that more or less reversible transitions occur along with the irreversible processes (reversible because the peaks always reappear). These thermograms were reproducible in several independent runs. There may be a wealth of information in the small reproducible peaks, which probably reflect different melting processes.

It is well known that higher heating rates will increase the "intensity" of heat flow at any temperature while decreasing the sensitivity. This is obvious considering that at higher heating rates, thermograms of kinetic events will be broadened in terms of temperature scale although the shape will be comparable in time scale regardless of heating rates. In other words, if peaks are overlapped in a narrow temperature range, slower heating rate run will enhance the separation of peaks. When peaks exhibit low intensity, higher heating rate runs will sharpen them and make them more obvious. The effect of heating rate on DSC thermograms is illustrated in Figures 4, 5 and considerably

simplified thermograms, compared to Figures 1 and 2, can be noted.

Samples for Figures 4 and 5 were not dried and the initial endothermic peaks observed at 60-240°C range were caused by water desorption. In Pittsburgh No. 8 coal, the irreversible transition in the 270-310°C range is more apparent than that observed at lower heating rate of 8 °C/min (Figure 1) and the temperature region of transition is increased by ca. 15°C at high heating rate of 30 °C/min, suggesting that the irreversible transition is an activated process. This would be expected for a glass transition. In Illinois No. 6 coal containing 7.97% moisture, the initial water endothermic peak is the dominant feature of the thermogram as could be expected from the high moisture content of this coal. Subtle changes in the subsequent runs for Illinois No. 6 coal are still visible in the difference DSC thermograms, as shown in Figure 5(b) for which temperature range 250-350°C was chosen for clarity. The downward (endothermic) trend above 300°C is most distinct in the (1st-2nd) and (1st-3rd) runs whereas the (2nd-3rd) run exhibits a smaller transition. Again, this shows the irreversible change occurs mainly during first heating.

The interpretation of the transitions revealed by in the DSC is aided greatly by a knowledge of the solvent swelling behavior of the coal as a function of temperature. Figure 6 shows a comparison of pyridine and THF swelling behavior of the Pittsburgh No. 8 coal obtained on the samples after DSC analysis (a single scan only). It is noted that there is an irreversible increase in THF swellability achieved in heating the coal to the range of temperatures 200-300°C. This is not accompanied by any significant weight loss. Nor is this change accompanied by any increase in pyridine swellability (in fact, a small decrease is seen, if anything). Pyridine is a stronger solvent, and can be expected to disrupt all noncovalent interactions in the coal. Pyridine reveals the extent to which the covalent network structure has been altered (or not altered) in the range of temperature cited above, since it is believed to be the most effective solvent for disrupting non-covalent interactions in the coal. The weaker THF is not as effective in removing all noncovalent crosslinks, as is evident in that it does not swell the coal as much (note the molecular sizes are quite similar for pyridine and THF). For Pittsburgh No. 8 coal, heating the coal to the range of temperatures 200-300°C apparently results in an irreversible removal of noncovalent crosslinks, but not much change in covalent crosslinks. This observation was reported previously by us [17]. This presumably occurs because the coal structure undergoes a glass to rubber transition in this temperature range, and once the structure is more flexible, it can relax to a new equilibrium configuration which is more easily swelled by THF. This effect is presumably related to the observation made by Larsen and coworkers [18] that the first cycle of a swelling in a good solvent such as pyridine normally involves an irreversible expansion of the network structure, due to structural relaxation. This transition is not evident in post-heating pyridine swelling of coals because the solvent alone is already effective at relaxing the structure without the need for heating. This is consistent with the results of Sakurovs [19], which showed pyridine to be as effective as heating with respect to creating "mobility"(at least in bituminous coals up to 86% C content).

The thermally induced relaxation during the first cycle of heating is thus taken to refer the T_g of the raw coal. The fact that repeated DSC scans reveal the transition to be stronger in the first scan than in any subsequent scans confirms the irreversible nature of the process that accompanies the glass transition. Again, a glass transition itself should, of course, not be irreversible. It is the release of stored strain energy that is irreversible. One can imagine that the thermally induced transition involves the disruption of aromatic stacking interactions formed under geological pressure. Since there is no comparable pressure applied when the sample is cooled in a DSC, the same interactions will not be restored; the thermodynamics has been changed.

Interestingly, Figure 6 shows that more time is required to reach THF swelling equilibrium for heat treatment temperatures below 300°C. This indicates that the accessibility of the coal is also irreversibly altered (increased) by heat treatment above this temperature (the structure swells more

readily to final equilibrium value above 300°C). Pyridine swelling ratio slightly decreased with time presumably by weight loss due to extraction of the coal by pyridine.

Figure 7 shows changes of the swelling ratio in THF against pyrolysis temperature for Illinois No. 6 coal along with the weight loss profile (the determination of the pyridine swelling profile against pyrolysis temperature for Illinois No. 6 coal is under way). In contrast to Pittsburgh No. 8 coal, Illinois No. 6 coal exhibits a drastically different THF swelling behavior with heat treatment temperature. Higher swelling ratio was obtained in the low temperature region (<300°C). The fact that Illinois No. 6 coal can swell significantly in THF without any heat treatment reflects a much different starting structure than that of Pittsburgh No. 8 coal. This clearly demonstrates the importance of coal composition in swelling. The swelling evidence to support the DSC interpretation is thus not as clear in Illinois No. 6 coal. The relatively small increase in swellability above 250°C is all that accompanies the transition identified by DSC. The swelling dynamics also suggest a small change at 250°C. Note that the highest swelling ratio is observed in 5 hours, and the ratio decreases with time. This is again presumably associated with a sudden increase in extractability at this temperature, and the swelling decreases as mass is removed. Presumably the increase in both swellability and extractability implies greater accessibility of the structure. From 350°C, pyrolytic crosslinking is clearly dominant as illustrated in the drop of THF swelling ratio and the increase in weight loss. Several pyridine swelling studies on bituminous coals [20] noted that pyridine swelling ratio starts to fall when the pyrolytic bond breakage commences. It should be noted from Figure 7 that the weight loss in the 150-300°C range was 10.3-10.9 wt%, which is clearly higher than the moisture content 7.97 wt% of this coal. This shows either that something other than moisture is being lost, or that an arbitrary drying procedure, such as the ASTM procedure, does not give the correct picture regarding possible moisture loss. This is also suggested by Figure 5(a), which shows "drying" well above 150°C.

Figures 8 and 9 illustrate the correlation between DSC thermograms obtained at 30 °C/min and solvent swelling profiles in two other coals. For Upper Freeport medium volatile bituminous coal, the main endothermic relaxation process starts from ca. 310°C (Figure 8(a)) while THF swelling ratio starts to shoot up around the same temperature (Figure 8(b)). Note that samples for swelling ratio experiments were in this case prepared in a wire-mesh pyrolyzer at 8 °C/min under nitrogen environment [17]. On the other hand, in Pocahontas No. 3 low volatile bituminous coal, the DSC difference thermogram exhibits a rather wider endothermic profile from ca. 230°C, which coincides with dramatic changes in pyridine and THF swelling profiles.

In the case of both the Upper Freeport and Pocahontas coals, swellability increases are difficult to separate from the onset of pyrolytic bond cleavage processes, as evidenced by rapid mass loss. The data certainly suggest that significant increases in swellability precede the period of rapid mass loss, which actually always seems to coincide with swellability decrease. It is difficult to unambiguously say that the data in hand argue for a physical transition prior to the commencement of bond cleavage processes. More work is planned to address this question. In any case, the solvent swelling data do correlate reasonably with the DSC data in terms of predicting increased structural mobility.

In summary, DSC confirms what was suspected from THF solvent swelling in the high volatile bituminous coals - that there is a glass transition in the range of temperature from about 230 to 300°C. This is lower than earlier reported values [11], but it is understandable that some variation might be due to sample differences, heating rates, and the difficulty of interpreting simple DSC scans without additional confirming data such as solvent swelling.

Conclusions

- DSC and solvent swelling techniques were applied to evaluate structural changes at low

temperature (<350°C) before any major pyrolytic bond breakage occurs. The results reveal the existence of reversible structural changes together with an irreversible transition, centered around 200-300°C in three high volatile bituminous coals.

- DSC thermograms appear to correlate with THF swelling ratio profiles, with regard to the information they convey on structural relaxation.

Acknowledgement

The work reported here was financially supported by the Department of Energy Contract No. DE-AC22-91PC91027. EMS also acknowledges the support of the Exxon Education Foundation.

References

1. Lynch, L.J.; Sakurovs, R.; Webster, D.S. *Fuel* **1988**, *67*, 1036.
2. Suuberg, E.M.; Lee, D.; Larsen, J.W. *Fuel* **1985**, *64*, 1668.
3. Solomon, P.R.; Serio, M.A.; Despande, G.V.; Kroo, E. *Energy & Fuels* **1990**, *4*, 42.
4. Yun, Y.; Meuzelaar, H.L.C.; Simmleit, N.; Schulten, H.-R. In *Coal Science II*; Schobert, H.H., Bartle, K.D., Lynch, L.J., Ed.; ACS Symposium Series 461; ACS: Washington, DC, 1991; Chapter 8, p 89.
5. Yun, Y.; Meuzelaar, H.L.C.; Simmleit, N.; Schulten, H.-R. *Energy & Fuels* **1991**, *5*, 22.
6. Mahajan, O.P.; Tomita, A.; Walker, P.L., Jr. *Fuel* **1976**, *55*, 63.
7. Mahajan, O.P.; Tomita, A.; Nelson, J.R.; Walker, P.L., Jr. *Fuel* **1977**, *56*, 33.
8. Hefta, R.S.; Schobert, H.H.; Kube, W.R. *Fuel* **1986**, *65*, 1196.
9. Janikowski, S.K.; Stenberg, V.I. *Fuel* **1989**, *68*, 95.
10. Elder, J.P.; Harris, M.B. *Fuel* **1984**, *63*, 262.
11. Lucht, L.M.; Larson, J.M.; Peppas, N.A. *Energy & Fuels* **1987**, *1*, 56.
12. Hall, P.J.; Larsen, J.W. *Energy & Fuels* **1991**, *5*, 228.
13. Isaacs, L.L.; Tsafantakis, E. *Prepr. Pap.- Am. Chem. Soc., Div. Fuel Chem.* **1987**, *32(4)*, 243.
14. MacDonald, R.A.; Callanan, J.E.; McDermott, K.M. *Energy & Fuels* **1987**, *1*, 535.
15. Vorres, K.S. *User's Handbook for the Argonne Premium Coal Sample Program*; Argonne, Illinois, 1989.
16. Otake, Y.; Suuberg, E.M. *Fuel* **1989**, *68*, 1609.
17. Suuberg, E.M.; Otake, Y.; Deevi, S.C. *Prepr. Pap.- Am. Chem. Soc., Div. Fuel Chem.* **1991**, *36(1)*, 258.
18. Larsen, J.W.; Mohammadi, M. *Energy & Fuels* **1990**, *4*, 107.
19. Sakurovs, R.; Lynch, L.J.; Barton, W.A. *Prepr. Pap.- Am. Chem. Soc., Div. Fuel Chem.* **1989**, *34(3)*, 702.
20. Ibarra, J.V.; Moliner, R.; Gavilan, M.P. *Fuel* **1991**, *70*, 408.

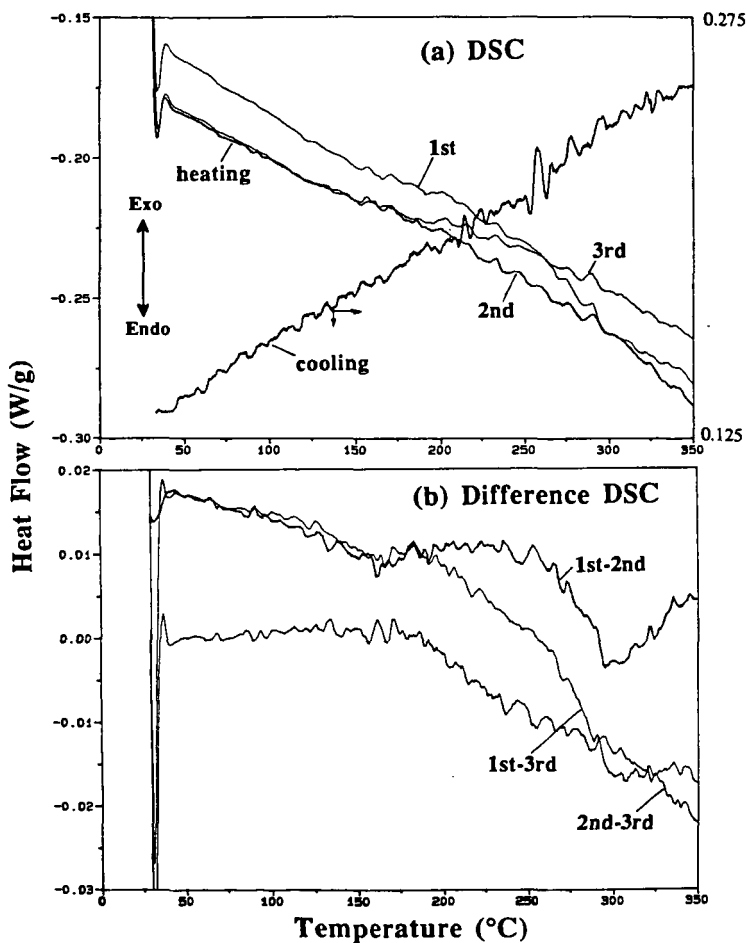


Figure 1. DSC and difference DSC thermograms for Pittsburgh No. 8 coal. After drying coal at 150°C in the DSC, DSC runs were repeated three times at 8 °C/min for the same sample. Difference thermograms in (b) were obtained by subtracting two thermograms in (a).

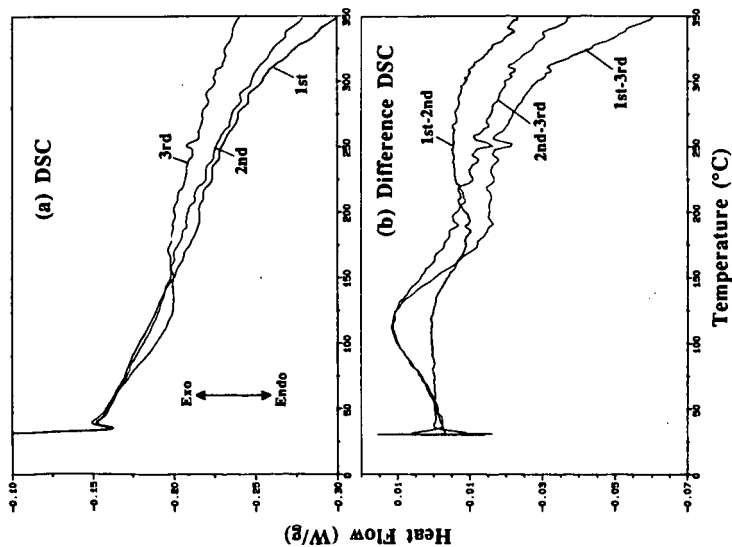


Figure 2. DSC and difference DSC thermograms for Illinois No. 6 coal. After drying coal at 150°C in the DSC, DSC runs were repeated three times at 8 °C/min for the same sample. Difference thermograms in (b) were obtained by subtracting two thermograms in (a).

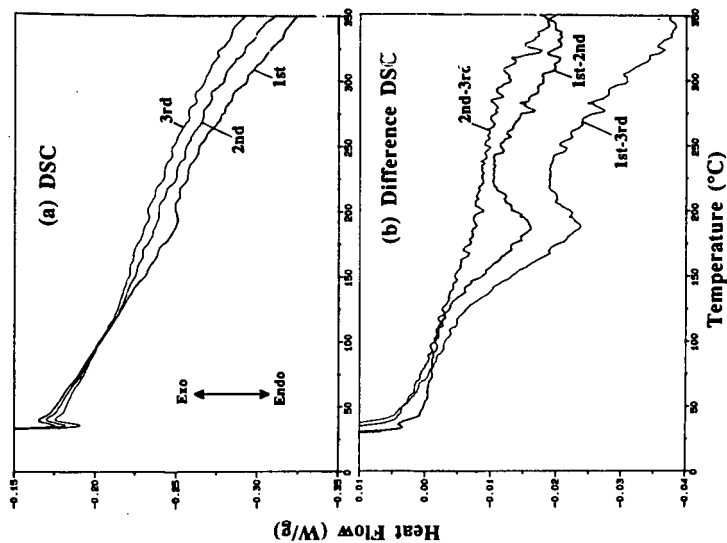


Figure 3. DSC and difference DSC thermograms for Blind Canyon coal. After drying coal at 150°C in the DSC, DSC runs were repeated three times at 8 °C/min for the same sample. Difference thermograms in (b) were obtained by subtracting two thermograms in (a).

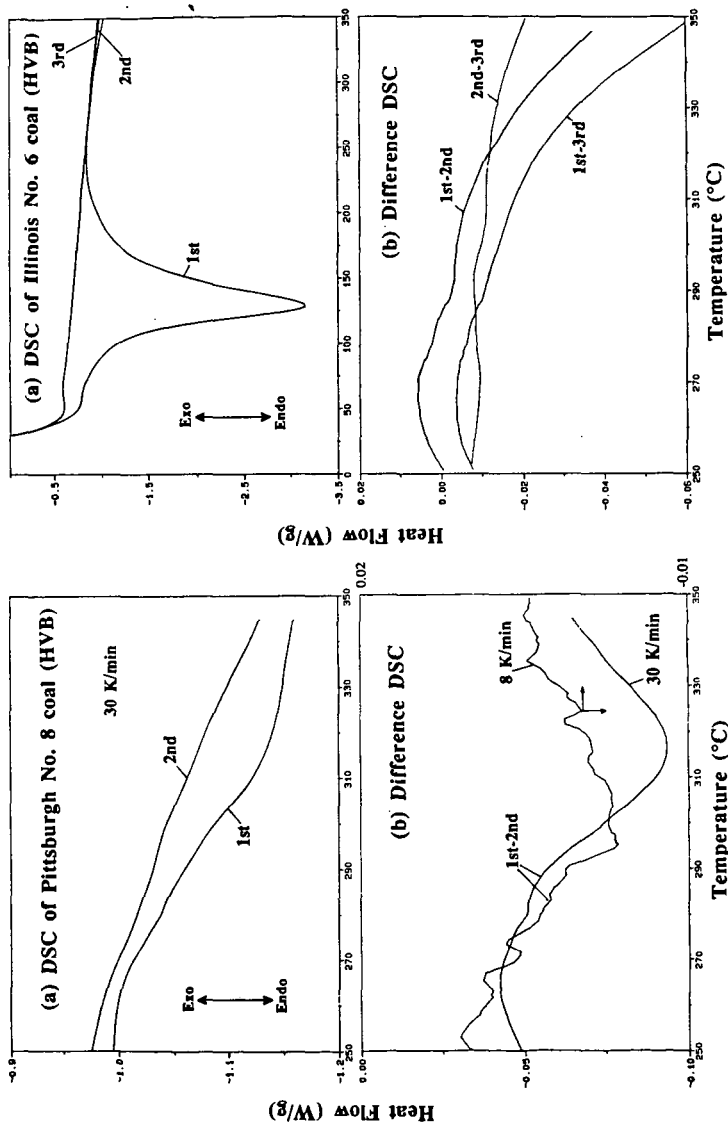


Figure 4. DSC and difference DSC thermograms for undried Pittsburgh No. 8 coal obtained at 8 °C/min and 30 °C/min.

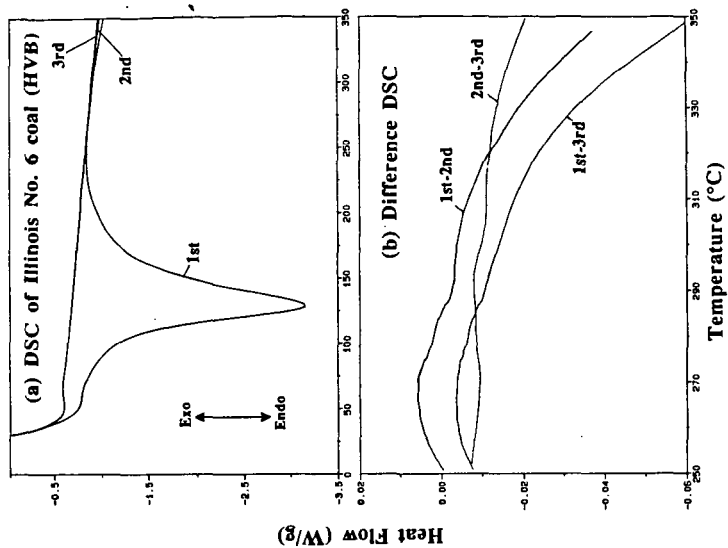


Figure 5. DSC and difference DSC thermograms for undried Illinois No. 6 coal obtained at 30 °C/min.

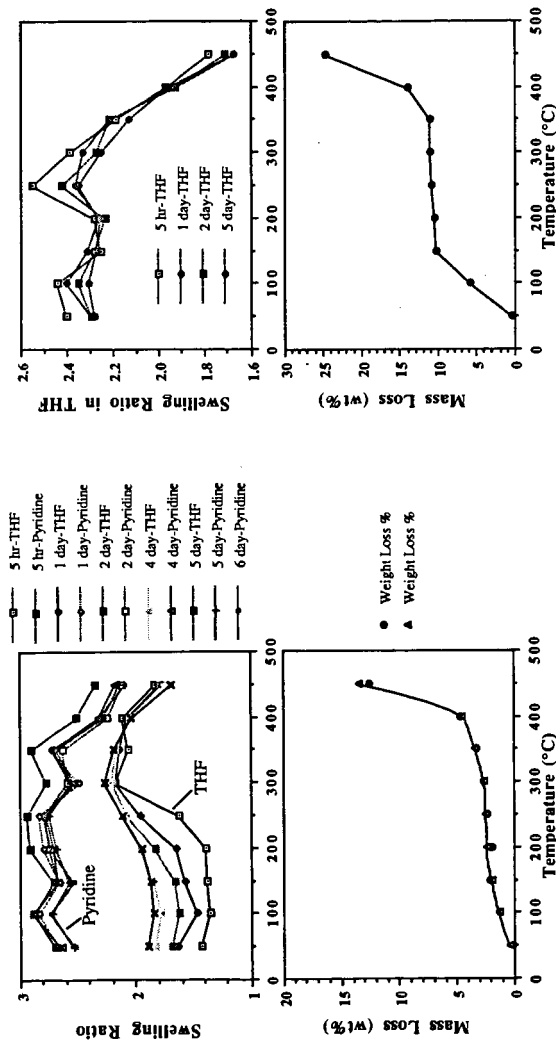


Figure 6. Changes of swelling ratio in tetrahydrofuran and pyridine as well as weight loss profile against pyrolysis temperature for Pittsburgh No. 8 coal (<20 mesh). Undried samples were placed in the DSC cell and heated at 8 °C/min under 90 ml/min nitrogen flow up to the specified temperature.

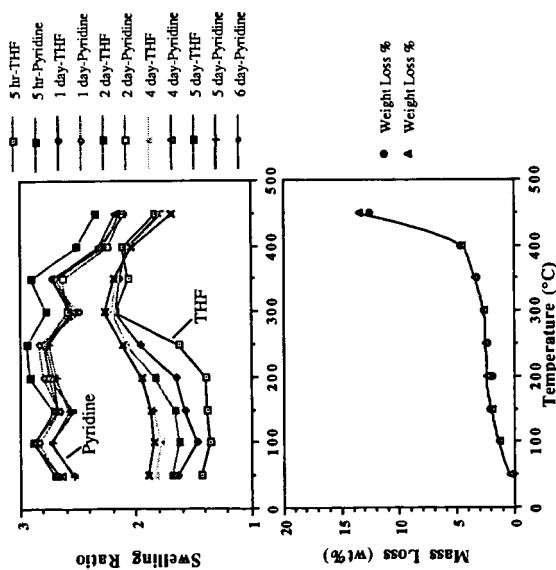


Figure 7. Changes of swelling ratio in tetrahydrofuran as well as weight loss profile against pyrolysis temperature for Illinois No. 6 coal (<20 mesh). Undried samples were placed in the DSC cell and heated at 8 °C/min under 90 ml/min nitrogen flow up to the specified temperature.

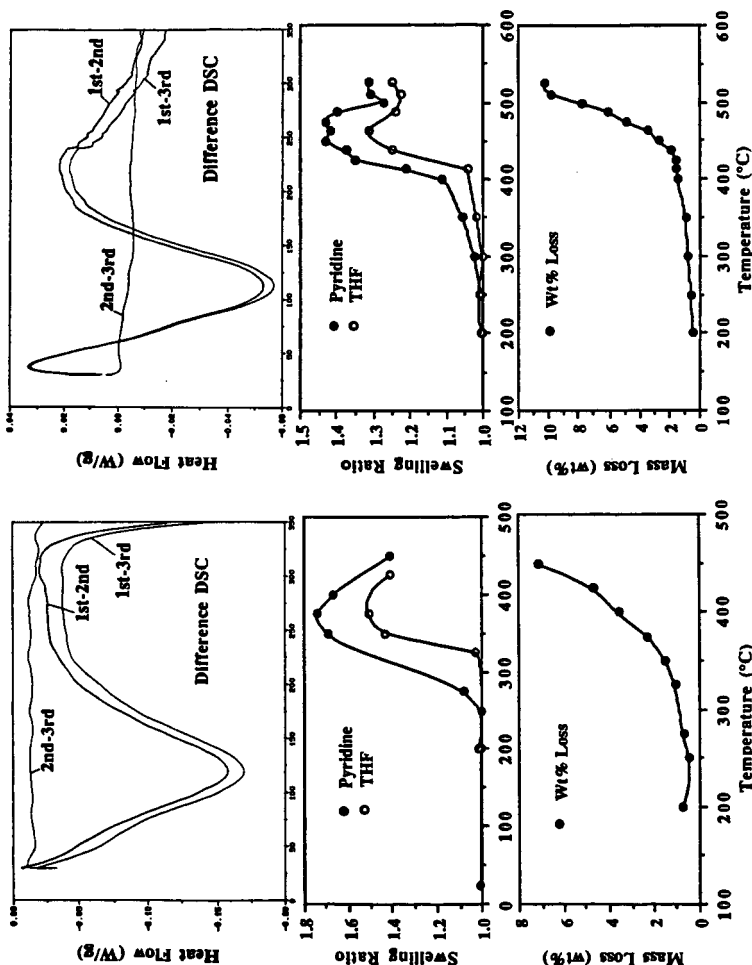


Figure 8. DSC difference thermograms as well as profiles of swelling ratio and weight loss for Upper Freeport medium volatile bituminous coal (-100 mesh). Note that DSC was performed at 30 °C/min whereas samples for swelling were obtained from wire-mesh reactor at 8 °C/min.

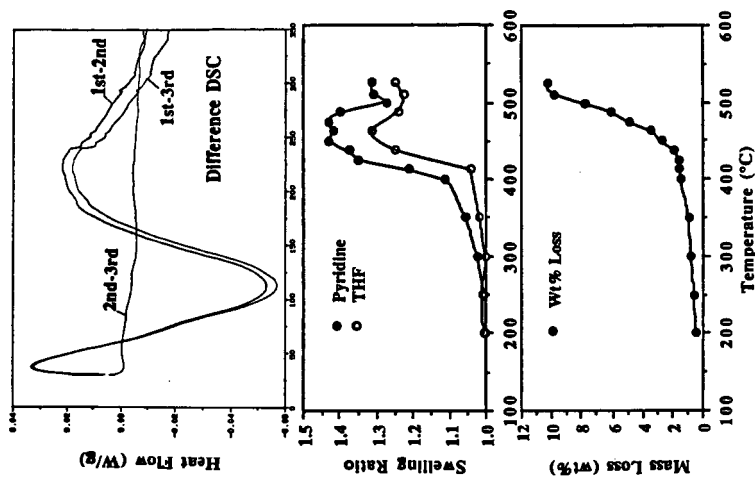


Figure 9. DSC difference thermograms as well as profiles of swelling ratio and weight loss for Pocahontas low volatile bituminous coal (-20 mesh). Note that DSC was performed at 30 °C/min whereas samples for swelling were obtained from the wire-mesh reactor at 8 °C/min.

Characterization of Coal-Derived Materials by Laser Desorption Mass Spectrometry*

J. E. Hunt, K. R. Lykke, and R. E. Winans
Chemistry Division
Argonne National Laboratory
Argonne, IL 60439

Keywords: laser desorption mass spectrometry, coal, maceral

ABSTRACT

Laser desorption time-of-flight mass spectrometry (LD/TOF MS) is used to characterize complex mixtures of large molecules derived from coals and separated coal macerals. Three groups of macerals, namely liptinite, vitrinite, and inertinite from Argonne Premium Coal Sample 7 were separated by a density gradient technique and subjected to small scale liquefaction. Samples of the maceral products were exposed to laser pulses from a XeCl-Excimer laser or the fourth harmonic output of a Nd:YAG laser. The general features of this method are the virtual absence of ion signal below m/z 200, a distribution of masses from m/z 200 to beyond m/z 1000 and reduced mass fragmentation in contrast to EI and FAB, where much fragmentation is present below m/z 200.

INTRODUCTION

The chemically and physically heterogeneous nature of coals dictates that their structure and reactivity patterns be complicated. The determination of the structural building blocks in coals is of crucial importance in research on their reactivity. The problem is complicated by the fact that the molecular structure of the organic part of coal is not dependent on a single molecule, but on a complex mixture of molecules that vary according to the type of coal. A number of complementary approaches have been used to investigate the structure of coal. Mass spectrometry has played an increasing role in characterizing the organic part of coals and coal-related materials. The approaches have varied from pyrolysis MS (pyMS) to fast atom bombardment (FABMS) to desorption chemical ionization mass spectrometry (DCIMS). Each of these approaches has particular strengths. For example, pyMS has shown heteroatom containing molecules and field ionization MS (FIMS) has produced molecular weight distributions of volatile tars^{1,2}.

Laser ablation techniques have been applied to coal characterization resulting in small molecules and in some cases fullerenes at high laser powers³⁻⁵. Our laser desorption (LDMS) study differs from previous laser ionization mass spectrometry studies. Our goal is to desorb ions characteristic of the molecular weight distribution present in the coal sample rather than to pyrolytically ablate material from the coal surface. The desorption laser is intentionally operated close to the ionization threshold to minimize any chance for fragmenting the desorbing material. In this paper the LD/TOF mass spectrometer is described and results on the molecular weight

*This work was performed under the auspices of the Office of Basic Energy Sciences, Division of Chemical Sciences, U.S. Department of Energy, under contract number W-31-109-ENG-38.

distributions of coal derived materials are presented. These data are also compared to other mass spectral methods.

EXPERIMENTAL

Coals

A complete discussion of the characteristics of the coals used in this study has been reported. Vacuum pyrolysis tars of Upper Freeport mv bituminous coal (APCS 1) are used to compare with other ionization techniques⁶. A coal selected for a second study was a high-volatile West Virginia bituminous coal from the Lewiston-Stockton Seam (APCS 7)⁷. In this study, three groups of macerals, namely liptinite, vitrinite, and inertinite were separated by a density gradient technique and subjected to small-scale liquefaction in tetralin. The products of the liquefaction were separated into light gases and hexane-soluble (oils), toluene-soluble (asphaltenes), and tetrahydrofuran-soluble (preasphaltenes) fractions. The LD/TOF data for the toluene solubles is presented here.

Lasers

The laser light source used for laser desorption is either a XeCl-excimer laser (308 nm, 10 ns pulse-width) or a Nd:YAG laser (266 nm, 200 ps pulse-width). The lasers are operated at a 1 to 100-Hz repetition rate at a constant fluence of approximately 10-100 mJ/cm², close to the ionization threshold to minimize fragmentation on the surface or in the gas phase. Focusing is accomplished with a 300-mm spherical lens for the desorption laser. Positioning of the desorption laser on the 1.5 cm diameter sample is aided by a He-Ne laser collinear with the desorption laser and a closed-circuit video image of the sample surface.

Mass Spectrometer

The instrument used here is a time-of-flight mass spectrometer constructed in-house. The mass spectrometer is established by a sample surface (a stainless steel polished surface), an acceleration field, x- and y-deflection fields, and field-free region with an ion detector at the end (Figure 1).

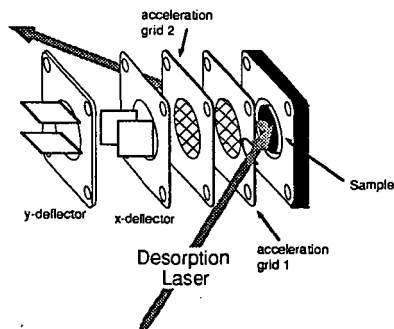


Figure 1. Schematic diagram of the ion-source region of the LD/TOF mass spectrometer.

This design is simpler than in conventional TOF instruments as the ionization source is already pulsed and therefore no pulsed acceleration voltage is needed. The resolution of the mass spectrometer is laser-pulse width limited with $m/\Delta m$ of approximately 400 FWHM for the 308 nm-pulse and 1500 for the 266 nm-pulse. The mass spectrometer includes vertical and horizontal deflection plates for ion beam steering, a set of pulsed-deflection plates for eliminating high-intensity low-mass ions and an Einzel lens system. The overall flight path length is 120 cm with acceleration distances of 4 mm for each of the two acceleration regions. Ions are produced at threshold irradiances to minimize fragmentation of the desorbing molecules. The ions thus formed are accelerated to 10 keV and detected using a dual-channelplate detector with a modest post-acceleration potential. Ion currents are recorded in a LeCroy 8828 transient recorder with a maximum time resolution of 5 ns or by single-pulse counting in a LeCroy 4208 time-to-digital converter with a time resolution of 1 ns. Further processing of the data is accomplished in a PC-based software system. The typical operating vacuum is 5×10^{-9} Torr.

The samples are prepared in a nitrogen-purged isolation box by allowing solutions of the soluble coal material to evaporate as thin films on the stainless steel sample probe. Approximately 50 μg of sample is placed on the probe. Less than 10^{-4} of the sample is consumed in a typical measurement. The remainder of the sample may be recovered intact following the measurement. LDMS spectra are produced by exposing the samples distributed as a thin layer on a stainless steel sample holder to the laser beam.

RESULTS AND DISCUSSION

The LD/TOF mass spectrum obtained from an Upper Freeport mv bituminous coal tar is shown in Fig. 2.

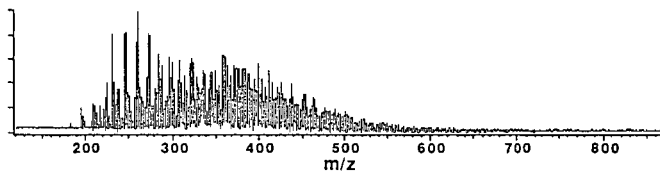


Figure 2. LD/TOF mass spectrum of Upper Freeport (APCS 1) vacuum pyrolysis tars.

The mass spectrum shows a virtual absence of ion signal below m/z 200. This is in contrast to EI and FAB, where much fragmentation is present below m/z 200. Several homologous ion series are present in the spectrum. A possible structure can be assigned to each of these series based on PyHRMS results from the same coal sample. The prominent series at $m/z=230$ to 272 with a Δm of 14 is assigned to alkyl-pyrenes or fluoranthenes. Another major series contains two different species, alkylphenylnaphthalenes and alkylhydroxy-pyrenes or fluoranthenes. In FAB MS the major cluster ions do not coincide with clusters seen in LD. The number average

molecular weight in the LD spectrum is 350. This compares favorably with DCI (325), while both FAB and FIMS show higher molecular weight distributions⁸. FAB and FIMS are known to be efficient in ionizing polar molecules and the higher molecular weight distributions may reflect a distribution skewed by minor amounts of higher molecular weight polar molecules.

The LD mass spectra of the toluene-soluble (asphaltenes) macerals are shown in Fig. 3.

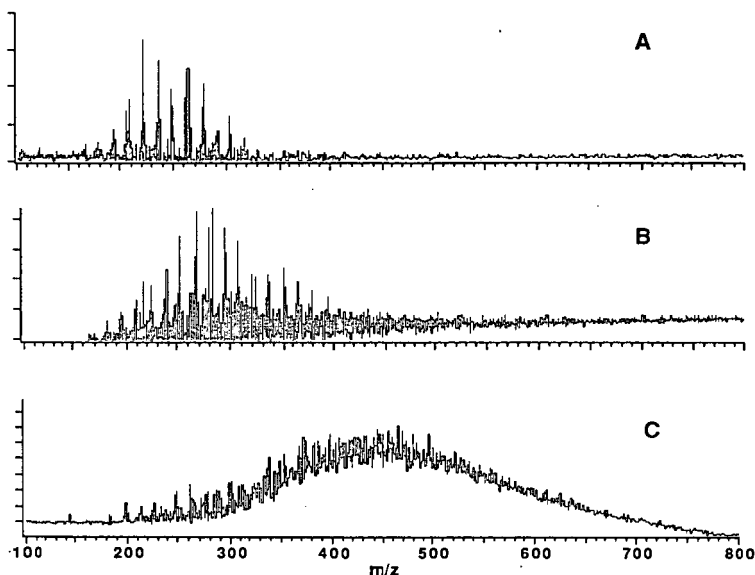


Figure 3. The LD/TOF mass spectra of toluene soluble (asphaltenes) macerals. A, liptinites; B, vitrinites; C, inertinites.

The three different maceral groups were placed in well-defined areas on a single sample probe for the mass measurement. The 200-ps 266-nm laser beam was then translated to each spot to ensure identical irradiance and desorption conditions. The first striking feature is that the LD/TOF data is consistent with carbon aromaticity and hydrogen content data. The most significant differences among the macerals are known to be their hydrogen content and carbon aromaticity⁷. The hydrogen content and the hydrogen/carbon ratio decrease in the order liptinite>vitrinite>inertinite, while the aromaticity shows the opposite trend. The inertinite, which is the least reactive maceral, is often thought to contain 'char-like material. It contains large multinuclear aromatic clusters. There is a clear trend of increasing average molecular weight of the ions with increasing carbon content (rank). This suggests that for a given irradiance LD/TOF is a good indicator of coal rank.

The LD/TOF MS of the liptinite (Fig. 3A) shows a single ion series separated by 14 amu extending from m/z 180 to 350. This alkyl type separation suggests a strong aliphatic methyl group content. This is supported by IR measurements. The number average molecular weight for the liptinite is 239. The vitrinite (3B) and the inertinite (3C) show increasing average molecular weights of 281 and 453. Note that the inertinite, which is thought to contain large multinuclear aromatic clusters, shows the broadest and least well-resolved spectrum. This implies a relatively low aliphatic content for the inertinite.

CONCLUSIONS

The mechanism at work in laser desorption of ions from surfaces is a subject of much speculation and conjecture. In spite of the complexity of the ionization mechanism, the fact remains that mass spectra of a large number of volatile organic compounds can be generated by laser desorption at threshold powers and that fragmentation of the parent molecule is minimal at best. Higher laser fluences may alter the ionization process to result in destructive fragmentation, in structurally significant fragmentation, or even ion-molecule reactions. Our goal here is to produce ions from the surface of coal-related samples with minimal fragmentation. For the coal products examined here, the LD/TOF mass spectra show no low m/z fragment ions and show molecular weight distributions that increase with rank. Although these are only preliminary experiments, the LD/TOF mass spectrometry approach to coal characterization looks promising with many variables in laser desorption conditions remaining to be explored.

REFERENCES

- (1) Winans, R. E.; Neill, P. H.; *Multiple-heteroatom-containing sulfur compounds in a high sulfur coal*, ACS Symposium Series 429: Washington, DC, 1990; Chapter 15, pp 249-259.
- (2) Schulten, H.-R.; Marzec, A. *Fuel* 1986, 65, 855-860.
- (3) Greenwood, P. F.; Strachan, M. G.; Willett, G. D.; Wilson, M. A. *Org. Mass Spectrom.* 1990, 25, 353-362.
- (4) Vastola, F. J.; Pirone, A. J. *Amer. Chem. Soc., Div. Fuel Chem., Preprints* 1966, 10, C53-C58.
- (5) Vastola, F. J.; McGahan, L. J. *Fuel* 1987, 66, 886-889.
- (6) Vorres, K. S. *Energy Fuels* 1990, 4, 420-425.
- (7) Joseph, J. T.; Fisher, R. B.; Masin, C. A.; Dyrkacz, G. R.; Bloomquist, C. A. A.; Winans, R. E. *Energy Fuels* 1991, Submitted.
- (8) Winans, R. E.; McBeth, R. L.; Hunt, J. E.; Melnikov, P. E. In *1991 International Conference on Coal Science*; University of Newcastle upon Tyne, UK, September 16-20, 1991, Submitted.

RAPID ANALYSIS USING DIRECT SAMPLING MASS SPECTROMETRY*

Michelle V. Buchanan, Robert L. Hettich, and Marcus B. Wise
Analytical Chemistry Division, Building 4500-S
Oak Ridge National Laboratory
Oak Ridge, TN 37831-6120

Key Words: Ion trap mass spectrometry; crude oil characterization; rapid analysis

INTRODUCTION

Mass spectrometry instrumentation has undergone substantial changes recently due to the advent of trapped ion techniques such as Fourier transform ion cyclotron resonance mass spectrometry¹ (commonly referred to as FTMS) and rf quadrupole mass spectrometers². The introduction of these highly versatile instruments have opened up exciting new applications of mass spectrometry to environmental measurements, biomolecule characterization, molecular dosimetry, materials science, and others. We have been investigating the use of quadrupole ion traps for the rapid, sensitive detection of compounds in a variety of matrices, including water, soil, air, oils, food, and physiological media. In these studies, methods for the direct introduction of the analyte into the quadrupole ion trap have been developed which require little or no sample preparation steps, resulting in analysis times of about 3 minutes and detection limits commonly in the low picogram range. In this paper, applications of this new analytical approach to the characterization of fossil-derived fuels will be described.

EXPERIMENTAL

A Finnigan ion trap mass spectrometer (ITMS) was used in these studies and was specially modified with an electropolished vacuum chamber and two 330 L/sec turbomolecular pumps to increase pumping speed and reduce background signals. Samples are placed in a 40 mL glass vial and closed with a teflon-lined septum screw cap fitted with two lengths of 1/16 inch tubing. One length of tubing extends to near the bottom of the vial and is used to introduce a flow of helium purge gas. The other length of tubing extends just beneath the vial cap and is used to transport the purged materials into the ITMS. The oil samples were diluted in methylene chloride/methanol and a few microliters of the resulting solution was spiked into distilled water. Water was used as the chemical ionization reagent.

For the gas chromatographic studies, a Hewlett-Packard 5990 GC was employed with a flame ionization detector. An aliquot of each oil sample diluted in methylene chloride was injected onto a 40 meter, DB-5 capillary column programmed to hold at 50 °C for 10 minutes, and then ramp to 280 °C at 5 °C/minute. Each chromatographic run took approximately 100 minutes.

For the combined gas chromatography/mass spectrometry studies, a Hewlett-Packard 5985 GC/MS was used. An aliquot of each oil sample in methylene chloride was injected onto a 30 meter, DB-5 capillary column programmed to hold at 50 °C for 5 minutes and then ramp to 280 °C at 20 °C/minute. Methanol was used as a chemical ionization (CI) reagent and was introduced through the direct insertion probe. A mass spectrum was taken every 3 seconds during the chromatographic run, with the entire GC run taking approximately 30 minutes.

Crude oil samples were obtained from the National Institute for Petroleum and Energy Research, Bartlesville, OK.

RESULTS AND DISCUSSION

A gas chromatograph equipped with a flame ionization detector was initially used to profile the twelve crude oil samples. Figure 1 shows chromatographic profiles of two oils, 90SPR53 (Iraq) and 75047 (Iran), and illustrates the hydrocarbon patterns observed for most of the oil samples. As expected, these oils consist mainly of aliphatic hydrocarbons (paraffins), with other minor components present. The chromatograms from

all of the samples were qualitatively quite similar and differed primarily in the abundance of the paraffins. Small differences in the minor components were observed in some cases, although the ability to differentiate the oils based only on this information was very difficult. In addition, the chromatographic analysis required 100 minutes.

In order to selectively examine the non-paraffin components of these oil samples, methanol chemical ionization GC/MS was used. Methanol chemical ionization permitted selective protonation of the alkyl aromatic hydrocarbons, alkenes, and heteroatom-containing hydrocarbons present in the samples, while eliminating ionization of the more abundant paraffins. The resulting mass spectra for these oils consisted primarily of alkyl aromatics, C_2 - to C_7 -benzenes and C_6 - to C_4 -naphthalenes, as shown in Figures 2 and 3, respectively. Selected ion chromatograms of the alkyl benzenes and alkyl naphthalenes revealed differences in the relative and absolute abundances of these components in the various oil samples, but the ion signal levels were quite low in most cases and may be difficult to reproducibly quantitate. In these GC/MS studies, because the alkyl aromatics were selectively detected and only classes of compounds were quantitated, less chromatographic resolution was required than in the GC FID studies and a faster column program was employed. However, the GC/MS analysis still required approximately 30 minutes.

Previous research in our laboratory has demonstrated the capability of purging volatile samples from an aqueous matrix directly into an ion trap mass spectrometer without chromatographic separation¹. This method, called direct sampling ion trap mass spectrometry (DS ITMS) has been used as a rapid, sensitive means of differentiating a series of fuels, including gasoline, diesel, and jet fuels. The volatile components from the oil are then purged from the solution with helium directly into the transfer line of the ITMS (no chromatographic separation is used). The effluent entering the ITMS is ionized using water chemical ionization (the water purged from the sample is used as the chemical ionization reagent). This method allows selective ionization of alkyl aromatics and heteroatom-containing hydrocarbons but not the paraffins. Using this approach, all the volatile components from the oils could be characterized with the total analysis requiring approximately 3 minutes, as compared to 30-100 minutes for the chromatographic analysis. In addition, the remarkable sensitivity and versatility of the ITMS provided detailed information on trace levels of compounds that are characteristic of each oil.

This same DS ITMS approach was adapted to differentiate the crude oil samples. Figure 4 illustrates the total ion purge profile and extracted ion profiles for C_2 -benzenes (m/z 107) and C_3 -benzenes (m/z 121) for oil 90SPR53. The entire experiment required approximately three minutes. Figure 5 represents the mass spectrum obtained approximately 2 minutes into the purge and reveals the ions observed from this sample. Ions at m/z 83, 85, and 96 originate from the solvent and are present in the blank. The ions with m/z 93, 107, 121, 135, and 149 arise from C_1 - to C_5 -alkyl benzenes present in the oil sample.

Table 1 is the resulting compilation of relative ion abundances for the alkyl aromatics from the 12 crude oils studied thus far by ITMS. Because the signal from C_2 -benzenes at m/z 107 was usually the most abundant, all other ion abundances were normalized to its intensity. The samples were run in duplicate (some were acquired in triplicate), and the precision of the measurements are also included in Table 1. From these data, it may be seen that differentiation of many crude oils is possible using these ion ratios. Note that oils 74023 and 69080 yield similar ion abundance ratios and that they are from the same oil field, but sampled in different years, 1974 and 1969, respectively. In some cases, however, even though the relative ion ratios are similar, the absolute abundances of the alkyl aromatics vary considerably. This is shown in the bar graph in Figure 6, where absolute abundances of the ion with m/z 107 is illustrated. In the case of 90SPR53 and 75047, where the ion abundance ratios in Table 1 prohibit clear distinction of the crude oils, the differences in the absolute abundances of m/z 107 permit their differentiation. In order to quantitatively compare absolute ion abundances, an internal standard (possibly deuterated xylene) should be added to the oil samples prior to analysis to provide a standard ion for comparison.

These low molecular weight alkyl aromatics may not be the best components for the identification process, however, because "weathering" of the oils could lead to losses from volatilization, changing the relative and absolute abundances of the monitored ions. Thermal desorption ITMS, another type of DS ITMS technique developed in our laboratory, could be used to examine the less volatile, higher molecular weight constituents

of the oils (e.g., naphthalenes, phenanthrenes, etc.), which should be less susceptible to "weathering". The thermal desorption method employs rapid heating of a small aliquot of the neat sample to analyze compounds with lower volatilities by ITMS.

CONCLUSIONS

In this study, the potential of DS ITMS for the rapid differentiation of crude oils was examined. Twelve Middle Eastern crude oils were analyzed by GC FID, GC/MS, and DS ITMS. The GC FID chromatograms, which required approximately 100 minutes each to acquire, were qualitatively quite similar, making differentiation of various oils difficult. GC/MS using methanol chemical ionization provided selective ionization of alkyl aromatics and heteroatom-containing hydrocarbons in the presence of aliphatic compounds. However, this technique requires approximately 30 minutes per analysis and generated ion signal levels which were quite low and were difficult to reproducibly quantitate. Some differences in the alkyl aromatic hydrocarbons ratios of the different oils were observed, however. Direct sampling ITMS, using water chemical ionization, of oil samples provided a rapid, sensitive method of examining the abundances of volatile components in the samples. Examination of the ion ratios of the alkyl aromatics provided differentiation for most of the oil samples. Further differentiation could be obtained by comparing absolute ion abundances. Addition of an internal standard, such as a deuterated xylene, would allow the absolute ion abundances to be determined more accurately. The DS ITMS technique required a total analysis time of only three minutes compared with 30 to 100 minutes for chromatography-based techniques.

REFERENCES

- ¹M. V. Buchanan and M. B. Comisarow, in "Fourier Transform Mass Spectrometry", American Chemical Society, ed. M. V. Buchanan, American Chemical Society, Washington, 1987, pp. 1-20.
- ²R. G. Cooks and R. E. Kaiser, Jr., *Acc. of Chem. Res.*, **23**, 213 (1990).
- ³M. B. Wise, M. V. Buchanan, and M. R. Guerin, "Rapid Determination of Target Compounds in Environmental Samples Using Direct Sampling Ion Trap Mass Spectrometry," Proceedings, 38th ASMS Conference on Mass Spectrometry and Allied Topics, June 3-8, 1990, Tucson, AZ, pp. 619-620.

*Research sponsored by the Space and Defense Technology Program, Martin Marietta Energy Systems, Inc., under contract DE-AC05-84OR21400 with the U.S. Department of Energy.

"The submitted manuscript has been authored by a contractor of the U.S. Government under contract No. DE-AC05-84OR21400. Accordingly, the U.S. Government retains a nonexclusive, royalty-free license to publish or reproduce the published form of this contribution, or allow others to do so, for U.S. Government purposes."

Table 1. Low Abundance Ratios for Twelve Middle Eastern Crudes Determined by DS ITMS				
Oil Sample ID*	121 107	135 107	149 107	93 107
90SPR53 ^a	0.90 ± .02	0.49 ± .03	0.09 ± .01	0.58 ± .02
75047 ^b	0.89 ± .02	0.51 ± .02	0.15 ± .01	0.68 ± .05
70007 ^c	0.91 ± .03	0.51 ± .02	0.11 ± .006	0.62 ± .05
67066 ^d	0.91 ± .03	0.61 ± .01	0.15 ± .004	0.71 ± .05
70070 ^d	0.85 ± .002	0.50 ± .01	0.09 ± .01	0.75 ± .003
69068 ^e	0.87 ± .02	0.52 ± .01	0.12 ± .02	0.66 ± .04
72022 ^e	1.23 ± .02	0.85 ± .02	0.23 ± .02	0.73 ± .001
74023 ^{b**}	0.82 ± .02	0.47 ± .02	0.11 ± .001	0.68 ± .03
69080 ^{b**}	0.80 ± .01	0.45 ± .03	0.10 ± .002	0.73 ± .01
69085 ^b	0.76 ± .01	0.35 ± .01	0.07 ± .004	0.74 ± .02
69086 ^b	0.72 ± .01	0.40 ± .02	0.11 ± .03	0.87 ± .10
70113 ^b	0.83 ± .001	0.42 ± .02	0.10 ± .02	0.68 ± .02

Country of Origin: ^aIraq, ^bIran, ^cUnited Arab Emirates, ^dSaudi Arabia, ^eKuwait

*Identities assigned by National Institute for Petroleum and Energy Research,
Bartlesville, OK.

**Oil from same field, but one sampled in 1974 and other in 1969.

Figure 1. Gas Chromatographic Profiles of Two Crudes. Total Analysis Time 100 Minutes.

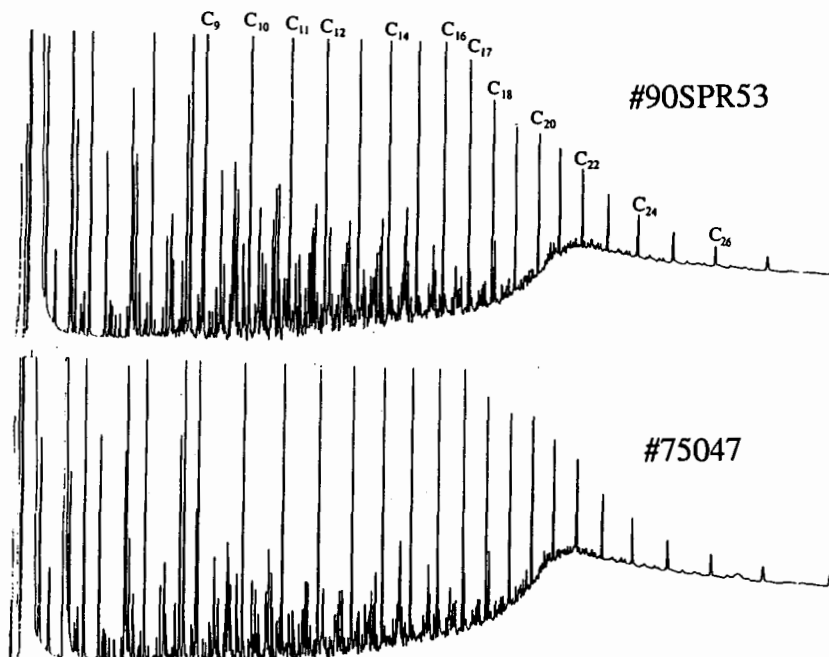


Figure 2. Extracted Ion Chromatograms for C₂-C₇ Alkyl Benzenes from Oil #90SPR53 Obtained by Methanol CI GC/MS.

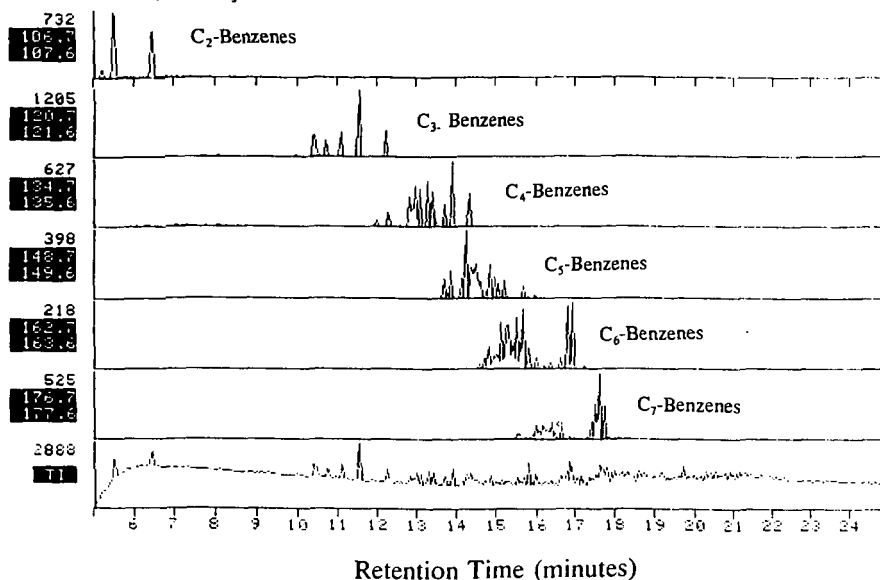


Figure 3. Extracted Ion Chromatograms for C₀-C₄ Alkyl Naphthalenes from Oil #90SPR53 Obtained by Methanol CI GC/MS.

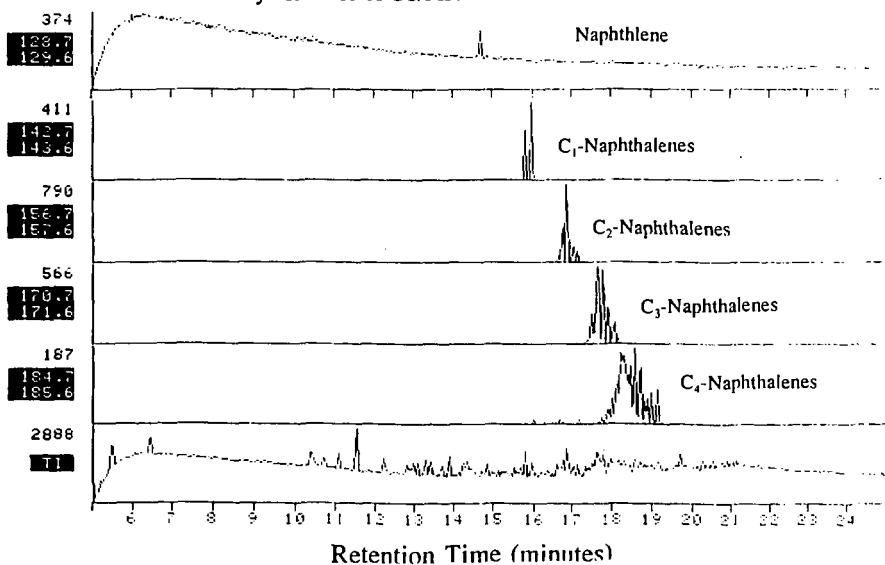


Figure 4. DS ITMS Purge Profile for Oil 90SPR531, Water CI.

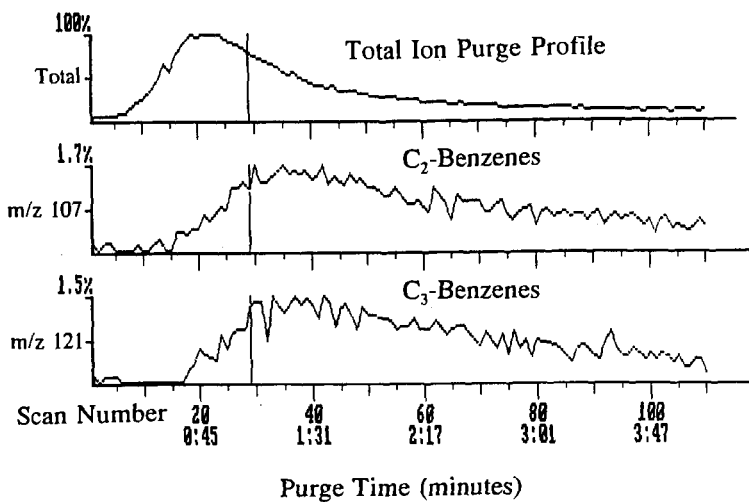


Figure 5. Water CI Mass Spectrum Taken 2 Minutes Into Purge Shown Above.

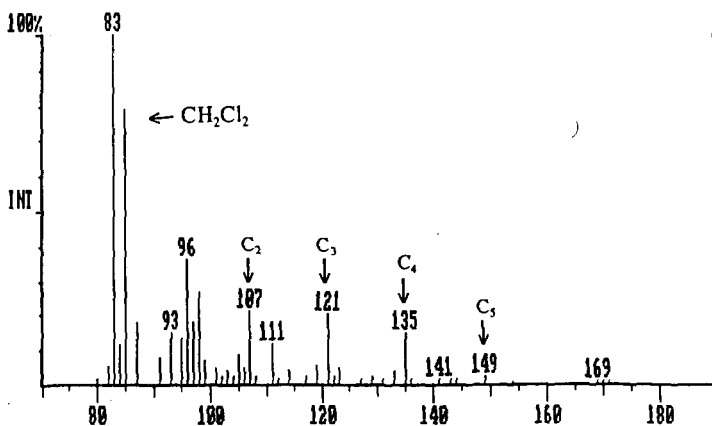


Figure 6. Absolute Abundance m/z 107. Direct Purge ITMS.

